Article:
Ihli, J, Wang, YW, Cantaert, B et al. (5 more authors) (2015) Precipitation of Amorphous Calcium Oxalate in Aqueous Solution. Chemistry of Materials, 27 (11). 3999 - 4007. ISSN 1520-5002

https://doi.org/10.1021/acs.chemmater.5b01642

Precipitation of Amorphous Calcium Oxalate in Aqueous Solution

Johannes Ihli[1]*, Yun-Wei Wang[1], Bram Cantaert[1], Yi-Yeoun Kim[1], David C. Green[1], Paul H. H. Bomans[2], Nico A. J. M. Sommerdijk[2] and Fiona C. Meldrum[1]*

[1] School of Chemistry, University of Leeds, Leeds, LS2 9JT, UK.

[2] Department of Chemistry and Chemical Engineering, Eindhoven University of Technology, Eindhoven, 5612 AZ ,NL

KEYWORDS: Calcium oxalate, amorphous, biomineralization, confinement

ABSTRACT

Inspired by the observation that crystalline calcium carbonate and calcium phosphate biominerals frequently form via amorphous precursors, a wide range of studies have been performed which demonstrate that many inorganic crystals can precipitate from solution via amorphous phases. This article considers the crystallization mechanism of calcium oxalate, which is a significant biomineral in many plants and the primary constituent of kidney stones in vertebrates, and shows that this can also precipitate via an amorphous precursor phase from aqueous solution. A range of approaches were employed to study calcium oxalate formation, including precipitation in bulk solution in the presence and absence of additives and in the spatially confined volumes offered by track etched membranes and a crossed cylinders apparatus. A freeze concentration method was also used to generate sufficient quantities of amorphous calcium oxalate (ACO) for analysis. The results show that amorphous calcium oxalate crystallizes rapidly in bulk solution, but can be significantly stabilized through the concerted activity of additives and confinement. We also demonstrate that ACO has a composition of $\approx CaC_2O_4{:}H_2O$. These data suggest that calcium oxalate biominerals, in common with their carbonate and phosphate counterparts, may also precipitate via amorphous phases.

INTRODUCTION

It is now widely accepted that crystalline calcium carbonate[1, 2, 3] and calcium phosphate[4, 5] biominerals often form via amorphous precursor phases. Employed by vertebrates, invertebrates and plants alike,[3, 5, 6] this strategy would appear to offer many advantages, such as access to more rapid mineralization rates and potentially greater control over the crystallization process. While it is recognized that some crystalline iron oxide biominerals, for example magnetite in magnetotactic bacteria and chiton teeth,[7] can form via the poorly-ordered phase ferrihydrite, there is as yet insufficient data available to determine whether this mechanism is common across the large number of known crystalline biominerals. Indeed, this can be a difficult question to answer, given the challenges associated with identifying amorphous materials when they are present in combination with crystalline phases and in characterizing biominerals that are only generated in small quantities.

Valuable insight into the possible mechanisms of formation of biominerals can therefore be gained by studying crystallization mechanisms in solution, as this gives the chance to study rapid reactions and to rigorously characterize products. While obviously not proving that the same mechanisms operate within biogenic systems, it is notable that organisms frequently retard processes as compared with the parallel reactions occurring in bulk solution, such that metastable polymorphs are commonly observed.[8, 9] This can be attributed to the action of soluble organic macromolecules, association with organic matrices and localization within confined volumes.[1, 10, 11, 12, 13, 14] Thus, observation of a crystallization pathway that goes through an amorphous phase provides strong evidence that this may also operate in biology. Conversely, identification of calcium sulfate hemihydrate identified as statoliths (gravity sensors) within deep-sea medusae[8] – where this polymorph of calcium sulfate had only been reported to precipitate from salt-free aqueous solutions at temperatures above 97 ^{o}C[15, 16] – prompted us to re-examine the mechanism of precipitation of calcium sulfate in solution, and revealed the presence of a previously unidentified amorphous calcium sulfate phase.[17]

In this paper we explore whether calcium oxalate (CaOx) can precipitate via an amorphous precursor phase in aqueous solutions, and identify the experimental conditions that extend the lifetime of amorphous calcium oxalate (ACO). Calcium oxalate is an important biomineral and is generated within specialised cells in many plants.[18] The crystals can form with a wide range of shapes and sizes and may provide structural support, or in the form of styloid and raphide crystals, as protection against predators.[19, 20] Precipitation of CaOx may also serve to maintain a low concentration of

oxalate within the cytoplasm. The formation of CaOx within vertebrates, in contrast, is typically pathological, and in humans is most commonly seen in kidney stones.[21] CaOx crystallizes in three forms, of which monohydrate (COM, CaC_2O_4:H_2O) is the thermodynamically most stable, and the dihydrate (COD, CaC_2O_4:$2H_2O$) and trihydrate (COT, CaC_2O_4:$3H_2O$) are metastable. CaOx in plants commonly appears as COM or COD,[22] while kidney stones are principally COM.[23, 24] Interestingly, a recent report has also shown that CaOx can be precipitated in an amorphous form from ethanolic solutions.[25]

In our work we employ a range of methods that are known to kinetically stabilize amorphous precursor phases in solution – including the freeze-concentration of saturated solutions,[26] precipitation within confined volumes[11, 27, 28, 29] and precipitation in the presence of polyelectrolytes[30, 31, 32] – to aid the identification and characterization of amorphous precursor phases of calcium oxalate in solutions. These methods demonstrate that amorphous calcium oxalate (ACO) particles with compositions of $\approx CaC_2O_4$:H_2O can form in aqueous solution, and that this amorphous phase can be significantly stabilized both in the presence of anionic polyelectrolytes and within confined volumes. That both of these conditions are characteristic or biomineralization processes suggests that calcium oxalate biominerals could well form via an amorphous phase, but that the challenges associated with characterizing calcium oxalate (it readily decomposes during analysis)[33] may have precluded the identification of this phase.

RESULTS

Bulk Precipitation

The possibility of observing amorphous calcium oxalate (ACO) in bulk solution was investigated by characterizing the precipitants formed by direct combination of equal volumes of $Na_2C_2O_4$ and $CaCl_2$ to give a final concentration of [CaOx] = 0.125-50 mM and pH of 6.8-7.05, where this procedure is consistent with those used in the preparation of ACC and ACP.[34, 35] These solutions were degassed with nitrogen for 2 hours prior to use to avoid the possible formation of calcium carbonate, due to influx of CO_2 into the solution from the atmosphere, and all precipitates were analyzed within 5-45 mins. In all cases the crystals were imaged using scanning electron microscopy (SEM), and the polymorph was identified by IR spectroscopy and Raman spectroscopy. The FTIR spectra of calcium oxalate monohydrate (COM) and calcium oxalate dihydrate (COD) differ significantly in the region of OH stretching vibrations (3600–3000 cm^{-1}), where the sharp vibrational band at $\approx$3000 cm^{-1} provides

a fingerprint for COM.[36] Distinguishing features in Raman spectra are that COM possesses two defined stretching bands located at 1460 and 1490 cm^{-1}, whereas COD displays a single sharp band at ≈ 1475 cm^{-1} (Supporting Figure 1).

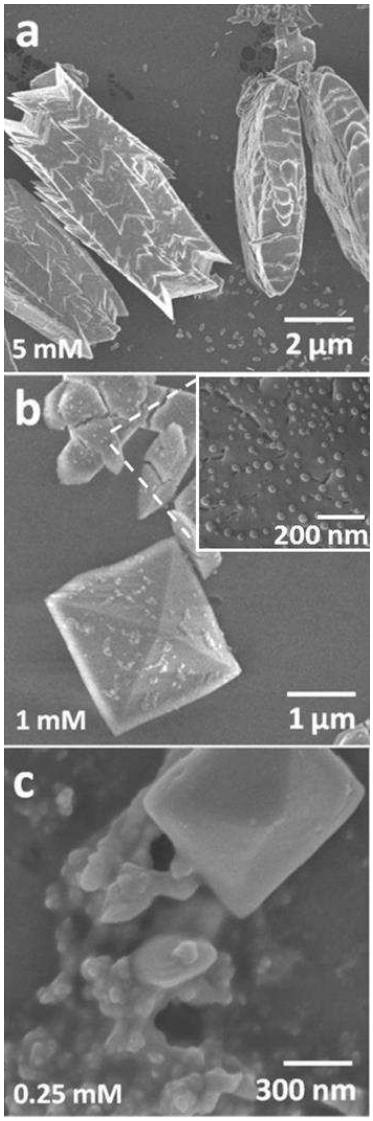

Figure 1. Electron micrographs of calcium oxalate precipitated in bulk solutions with concentrations of (a) 2.5 mM (COM), (b) 0.5 mM (COD + COM) and (c) 0.25 mM (COD). The inset in (b) shows small particles present on the surfaces of the COD crystals.

While the expectation from these bulk experiments was to obtain a homogeneous population of ACO particles at early reaction times, this was not observed. Instead, COM and/ or calcium COD was identified, where their proportions depended on the initial reagent concentrations employed. COM was the principal polymorph formed at solution concentrations of 2.5 mM and above, where these crystals appear in the form of spindles (Figure 1a), while COD was observed at concentrations below 2.5 mM, appearing as octahedral crystals (Figure 1b). The proportion of

COD increased with decreasing supersaturation (Figure 1c), a kinetic effect.[37] These images also show an interesting feature in that nano-sized, hemi-spherical particles can be seen on the surface of some COM and COD crystals (inset, Figure 1(b)). Although these closely resemble known amorphous precursor phases of calcium carbonate and calcium phosphate, unique characterisation of these particles was not possible due to their proximity to large crystalline calcium oxalate particles.

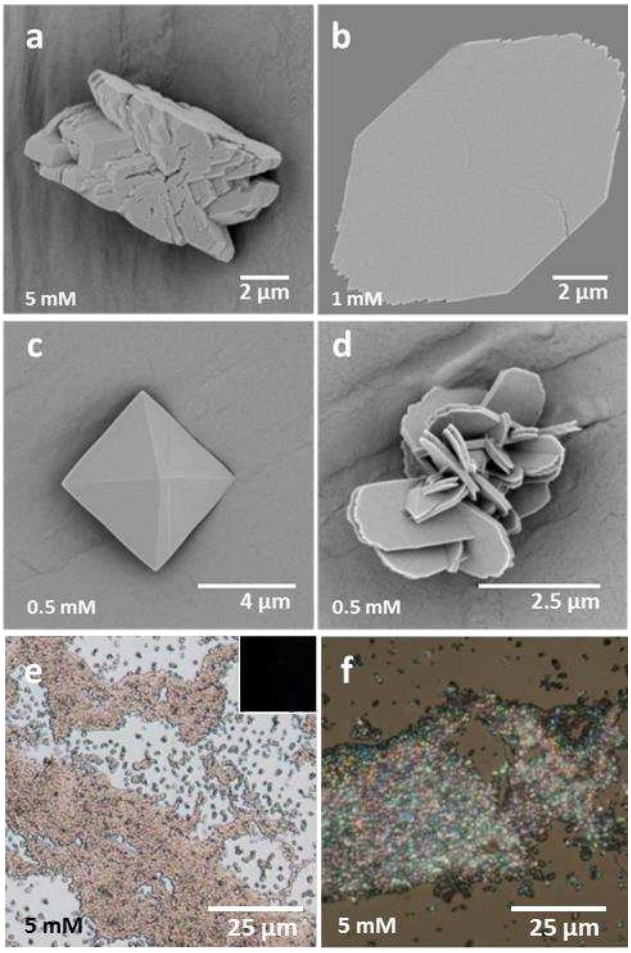

Figure 2. Electron micrographs of calcium oxalate precipitated in bulk solution in the presence of 50 µg ml^{-1} poly(acrylic acid) (PAA) at CaOx concentrations of (a) 2.5 mM (COM), (b) 0.5 mM (COM), (c) 0.25 mM (COM), (d) 0.25 mM (COD). (e) An optical micrograph of an area of thin film precipitated from a 2.5 mM solution, where the inset shows the appearance under crossed-polarizers. (f) The sample shown in (e) after heating to 180 °C, showing conversion to a polycrystalline thin film.

Attempts to stabilize ACO in bulk solution were therefore made by precipitating CaOx in the presence of poly(acrylic acid) (PAA). PAA is a proven crystal inhibitor for calcium oxalate,[38, 39, 40] and is well-recognized to stabilize amorphous calcium carbonate.[41] It is also commonly used as a synthetic analogue of the highly acidic macromolecules present within many biominerals.

Figure 2 shows micrographs of precipitates generated by from solutions of composition [CaOx] = 0.25-2.5 mM/ 50 μg ml^{-1} PAA (pH directly after mixing 6.6-6.8), where these show a marked change in precipitate morphology as compared to calcium oxalate formed in the absence of PAA. Pure ACO could not be extracted from these experiments, although small areas of amorphous thin films (Figure 2e) were detected on the mineralizing substrate in addition to individual crystals of CaOx (COM and COD) shown in Figure 2a. The amorphous character was identified as they were not visible under cross polarizers (inset, Figure 2e), and they dissolved within ≈ 30 mins in solution. Removal from solution and heating to 180 °C resulted in conversion to polycrystalline films (Figure 2f). These CaOx thin films also closely resemble those of calcium carbonate generated from polymer induced liquid precursor (PILP) phases in the presence of polyelectrolytes such as PAA, poly(aspartic acid) and poly(allylamine hydrochloride).[30, 31, 42] PILP is considered to act as a precursor to amorphous calcium carbonate.[14, 31, 32, 43] These data therefore strongly suggest that PAA supports the formation of an amorphous phase of calcium oxalate. Additional micrographs are provided in Supporting Figure 2.

Precipitation in Confined Volumes

Precipitation within confined volumes has been demonstrated to significantly stabilize amorphous calcium carbonate, calcium phosphate and calcium sulfate[11, 28, 29 44, 45] and was therefore also explored here as a means to stabilize ACO. Initial confinement studies employed a crossed cylinders apparatus, which is shown schematically in Figure 3. This apparatus provides a means of investigating how 1D confinement affects crystallization, and comprises two crossed half cylinders which are held in contact using a Teflon holder.[11] In the current experiments, glass tubes with diameters of 25 mm were cut to produce the half-cylinders and a TEM grid was placed between the two cylinders before they were brought into contact. An annular wedge is created between the glass surfaces, and the particular surface separation (h) between the crossed cylinder and TEM grid can be estimated according to $h \approx x^2/2R$.[11] R is equal to the radius of the half cylinder used and x is equal to the distance away from the contact point at surface separation (h). Precipitation of CaOx in this system was achieved by injecting 20 μl of a metastable crystal growth solution of concentration 1 mM (pH 6.82) between the half cylinders.

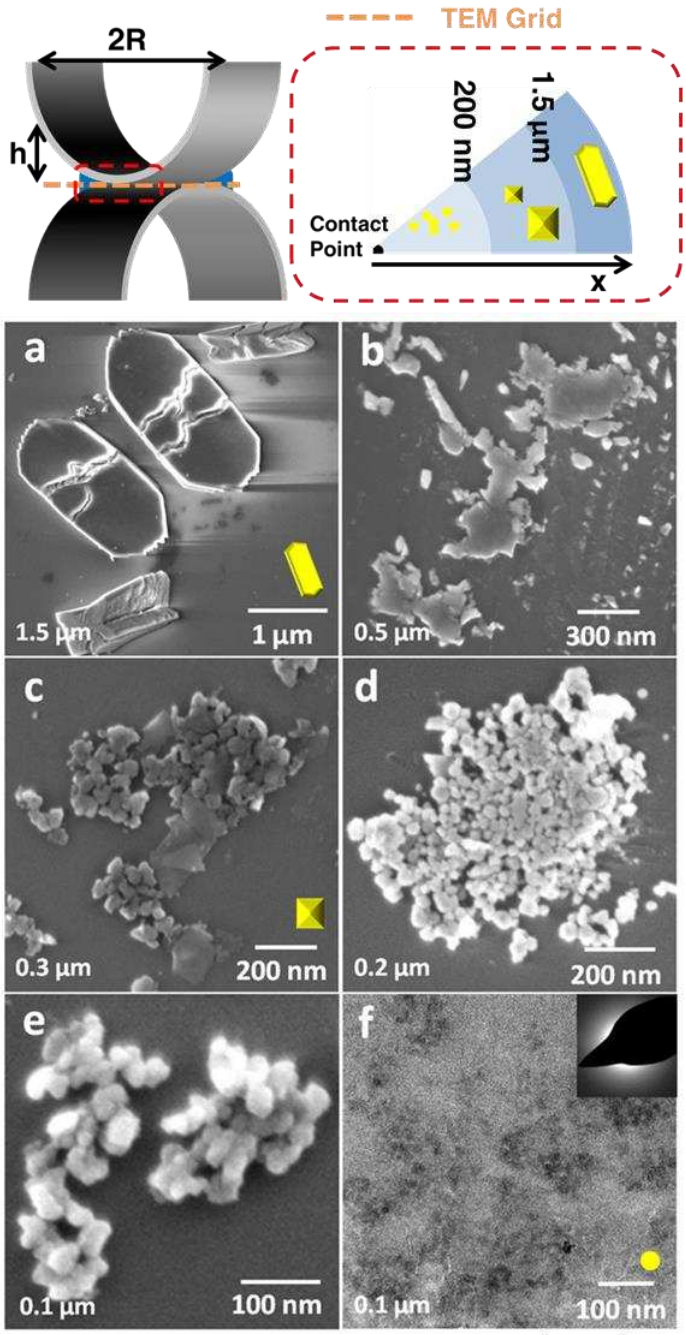

Figure 3. Calcium oxalate precipitation in a crossed-cylinders apparatus from a metastable crystal growth solution of concentration [CaOx] = 1 mM. The top images provide schematic representations of the experimental setup, where 2R is the diameter of the cylinder and h is the separation between a TEM grid placed between the cylinders and the glass surface. The correspondence with the crystal types seen at different surface separations are shown in the right hand figure. (a-e) Scanning electron micrographs and (f) transmission electron micrograph of precipitates generated at surface separations of (a) 1.5 µm (COM), (b) 0.5 µm (COD), (c) 0.3 µm (COD), (d) 0.2 µm and (e and f) 0.1 µm (ACO). The inset in (f) shows the corresponding electron diffraction pattern which confirms the amorphous nature of the precipitates formed close to the contact point.

All three forms of calcium oxalate – COM, COD and ACO – were observed within the crossed cylinders apparatus (Figure 3). COM was observed to be the dominant polymorph at surface separations greater than 1.5 μm (Figure 3a), while this was gradually replaced as the dominant polymorph by COD as the surface separation was reduced to 0.2 μm (Figures 3b and 3c), as confirmed by Raman spectroscopy. While the COM crystals showed morphologies typical of those formed in bulk solution, the COD crystals exhibited irregular forms, as reflects their formation in a constrained volume. Examination of surface separations less than 0.2 μm revealed the presence of small, spherical particles that were ≈ 10-50 nm in size (Figures 3d – 3f). These decreased in number density towards the contact point, due to the decreasing volume of reaction solution present. That these apparently "amorphous" particles were generated in isolation from other calcium oxalate forms enabled a more complete analysis to be performed using TEM and selected area electron diffraction (SAED). SAED patterns obtained from precipitates located close to the contact point at a surface separation of <0.1 μm returned an amorphous halo indicative of ACO (Figure 3f). In an attempt to confirm that these particles were amorphous, rather than there simply being insufficient material present to give a diffraction pattern, the particles were irradiated with the electron beam to try to induce crystallization. However, the particles decomposed rather than crystallized, as is consistent with the well-known radiation sensitivity of CaOx.[33] This behavior is likely to contribute to the fact that although there is an extensive literature on CaOx, an amorphous phase (formed in non-aqueous solutions) has only recently been identified.[25]

These experiments with the crossed cylinders apparatus provide very strong evidence for an amorphous CaOx phase, and demonstrate that confinement can be used as an effective route to stabilizing, and therefore identifying, metastable polymorphs. Due to the small amounts of CaOx generated, however, an alternative confinement system was also explored to enable conclusive identification of amorphous structure. CaOx was therefore precipitated within the pores of a track etched membrane (Figure 4a),[28, 46, 34] where this system generates much larger "individual" particles. In the set-up used, a 2 mM solution of $CaCl_2$ (pH 6.4) and a 2 mM solution of $Na_2C_2O_4$ containing 50 μg ml^{-1} PAA (≈ pH 7.7) were added, each to one arm, of a U-tube between which a 200 nm pore track etch membrane had been mounted. In this way, precipitation of CaOx occurs within the pores due to the cross diffusion of ions. PAA was employed in the system to facilitate infiltration of CaOx into the membrane pores, and to extend the lifetime of any amorphous phase. CaOx crystals were removed from the membrane pores

after either 12 hours or 2 weeks by dissolution of the membranes in dichloromethane and; electron micrographs of the resulting rods are shown in Figures 4b and 4c.

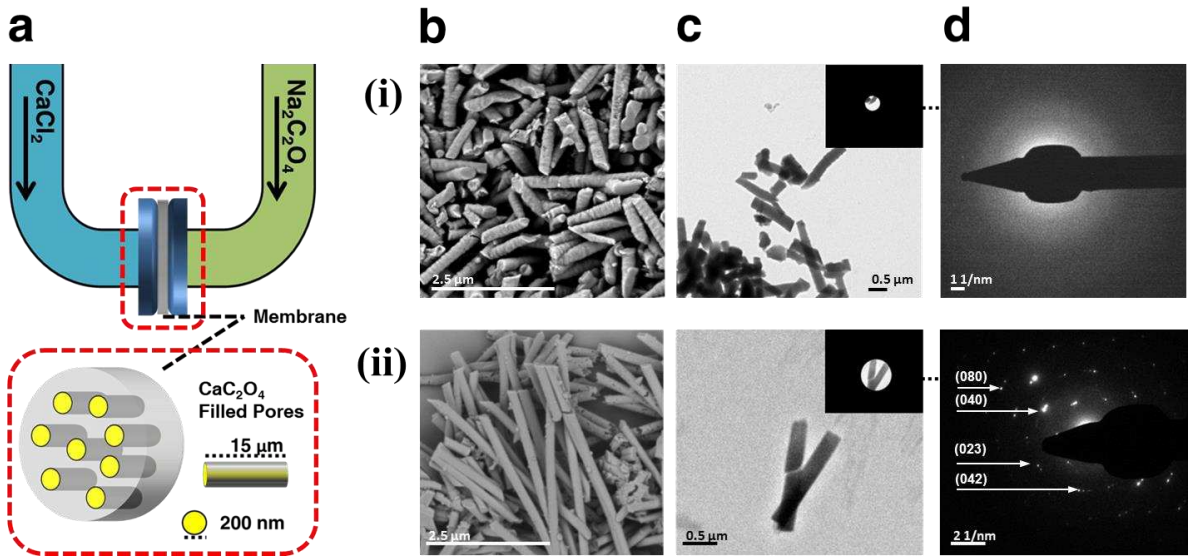

Figure 4. Calcium oxalate precipitated in the pores of track-etched membranes, where solutions of concentrations (2 mM $CaCl_2$) and (2 mM $Na_2C_2O_4$ and 50 µg ml^{-1} PAA) were placed in the respective U-tube arms. (a) Schematic representation of the experimental set-up used. (b-d) Analysis of rod-shaped particles precipitated and isolated from the membranes after (i) 12 hours and (ii) 2 weeks. (b) Scanning electron micrographs, (c) low dose transmission electron micrographs and (d) low dose selected area electron diffraction patterns corresponding to the rods shown in inset (c). (ii) The diffraction pattern corresponds to COM.

Well-defined rods with widths of ≈ 200 nm were obtained at both times, with those isolated after 12 hours being shorter than those isolated after 2 weeks (≈ 2 µm as compared with ≈ 4 µm). These rods were also analyzed using low dose cryo-TEM and low dose SAED, which showed that the "mature" rods were crystals of COM (Figure 4dii). Examination of the 12 hour rods (Figure 4di), by comparison, showed that they were amorphous. These ACO samples degraded rapidly under beam exposure even when low dose TEM was used for analysis (Supporting Figure 3), which further demonstrates the beam-sensitive character of CaOx. These experiments therefore provide a straightforward means of characterizing the crystallization pathway of CaOx in aqueous solution and conclusively show that amorphous CaOx can be generated as a precursor to the crystalline polymorphs.

Precipitation via Freeze Concentration

Having established that ACO can form in aqueous solutions, a freeze concentration method – which has previously been used to generate dry, counter-ion free amorphous calcium carbonate and amorphous calcium phosphate[26] – was explored to generate larger quantities for structural and compositional analysis. Pure ACO was obtained by rapid freezing and sublimation of saturated, counter-ion free CaOx solutions (pH ~7.1) (Figure 5).[26] Solvent removal during freezing of the saturated solution in liquid nitrogen induces precipitation due to the increase in supersaturation which occurs as the free solution volume decreases. The precipitate is then temporarily stabilized when the solution freezes completely, and is ultimately released as a dry powder on full sublimation of the ice. Electron micrographs of the CaOx precipitates generated by freeze-concentration are shown in Figure 6. The particles are approximately 40 nm in size and are similar in appearance to the ACO formed in bulk solution (Figure 1b) and in the crossed cylinders apparatus. Selected area electron diffraction of the ACO prepared by this method was featureless, displaying an amorphous halo (Figure 6).

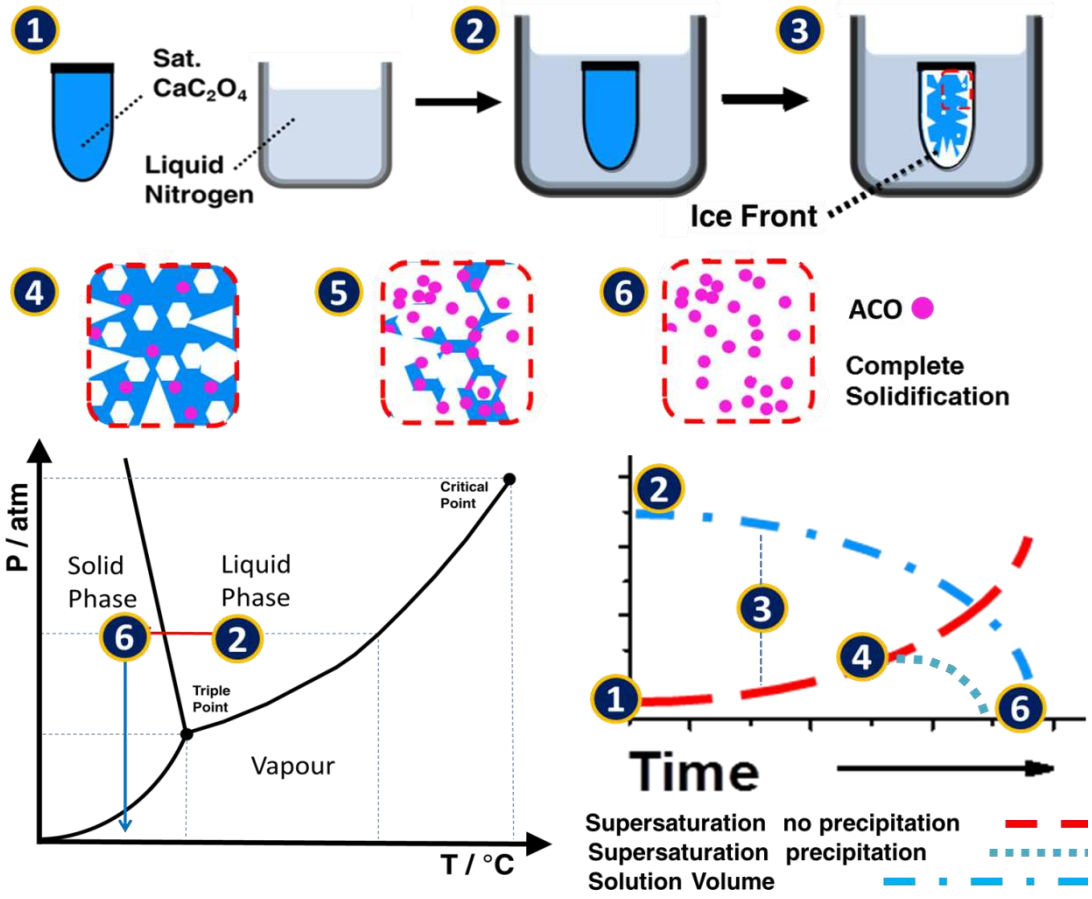

Figure 5. Schematic representation of the production of ACO by freeze concentration. Illustrated are the phase changes undergone by the solvent, where it converts from liquid to solid upon freezing (red arrow) and solid to gas during sublimation i.e. vacuum application (blue arrow). The changes which lead to ACO formation (Top) are shown as: (1) a saturated calcium oxalate solution is (2) plunged into liquid nitrogen (LN_2) (3) upon which the solvent begins to freeze, creating localized environments of increasing supersaturation. (4-5) This leads to ACO precipitation and finally (6) solvent solidification and ACO stabilization. These processes are also illustrated in line plots which show the suggested changes in supersaturation and solution volume accompanying the freezing of the solution.

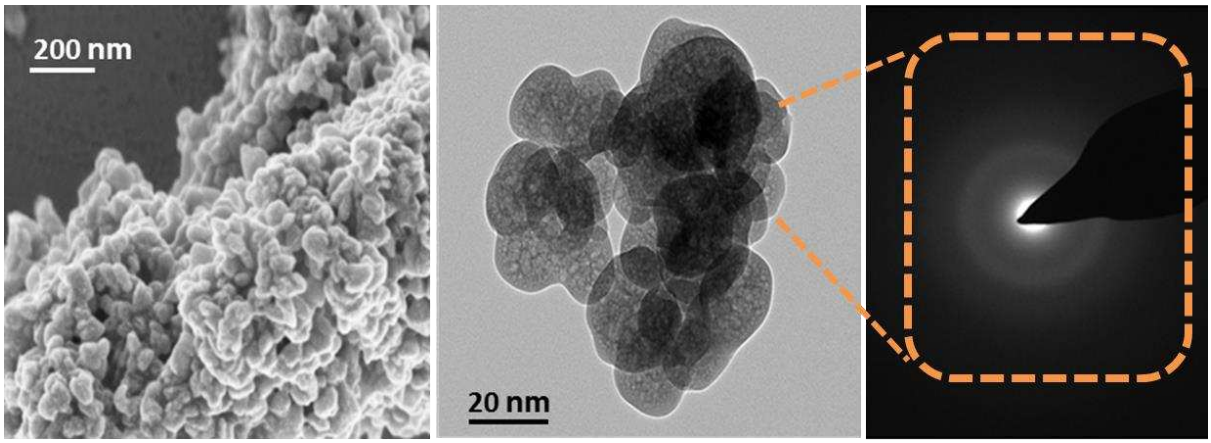

Figure 6. Amorphous calcium oxalate prepared by rapid freezing of a saturated solution of calcium oxalate. Given from left to right are SEM and TEM micrographs of the obtained ACO, where the electron diffraction pattern confirms the amorphous character of the formed precipitate.

Due to the volume of precipitate prepared by this method, it was possible to run full characterization by Raman microscopy, IR spectroscopy and thermogravimetric analysis (TGA). Particles were analyzed as-prepared and after two weeks storage in air, after when they had crystallized to COM. As comparison of the two spectra demonstrates, Raman spectra (Figure 7a) of the as-prepared ACO displayed broader peaks and single peaks corresponding to C=O asymmetric stretching modes at ≈ 1490 cm^{-1} and symmetric stretching modes located at ≈ 505 cm^{-1} (deformation of CO_2), as recently observed for ethanolic ACO.[25] These compare with the split peaks shown for these modes in COM. Both broadening and peak mergence are indicative of increased structural disorder. Figure 7b shows the IR spectra of the as-prepared ACO, which reveals the presence of structurally-disordered H_2O (≈ 3300 cm^{-1}). Structuring of the H_2O molecules occurs on crystallization to COM, as is evident in the more defined appearance of the

≈ 3300 cm^{-1} band, which comprises multiple vibration peaks. The peak at 1160 cm^{-1} can be attributed to a silica impurity. Overall, however, the IR and Raman spectra of ACO are not sufficiently different from those of COD and COM to enable conclusive polymorph identification.

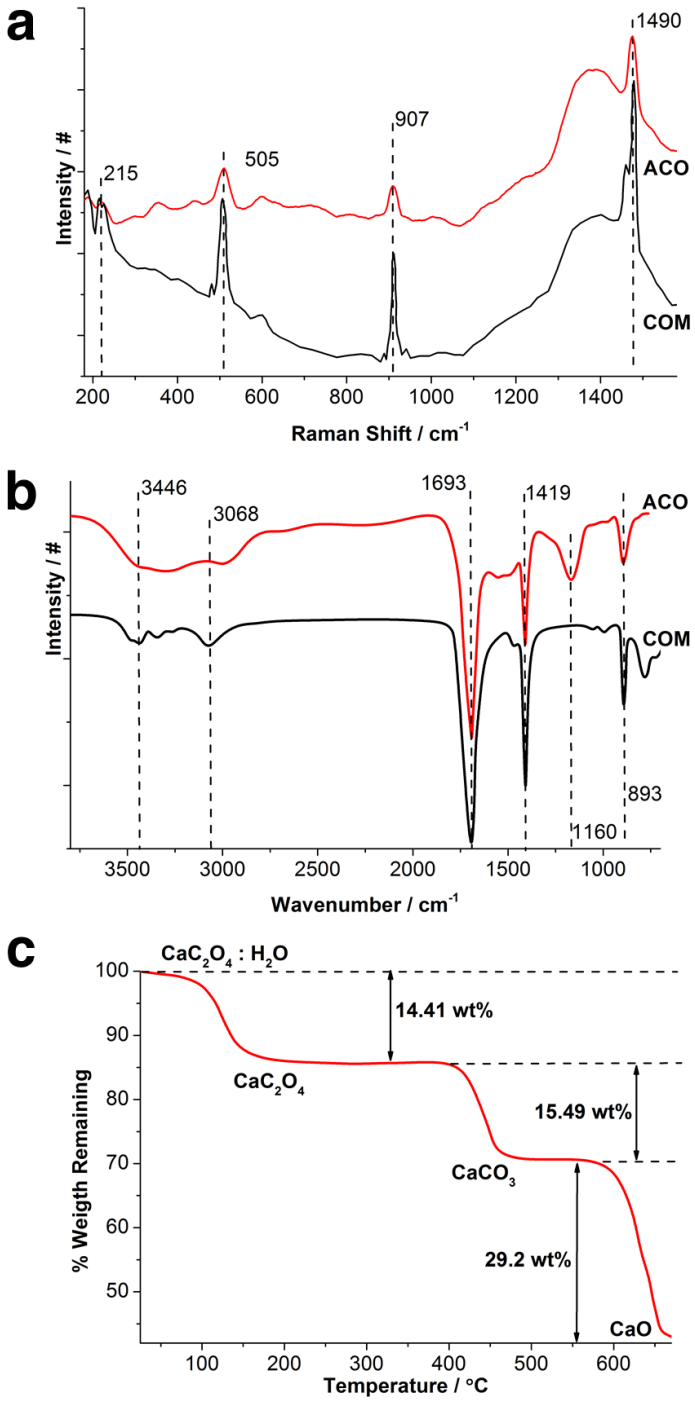

Figure 7. Amorphous calcium oxalate prepared by rapid freezing of a saturated solution of calcium oxalate. (a) Raman and (b) IR spectra of the obtained ACO, together with spectra obtained after the ACO had crystallized in air. (c) Thermogravimetric analysis (TGA) of the obtained ACO, showing the stepwise decomposition of formed hydrated precipitate to dehydrated calcium oxalate, calcium carbonate and eventual calcium oxide with increasing temperature.

Thermogravimetric analysis (TGA) of the prepared ACO (Figure 7c) was also performed to gain information on the composition of this material, and revealed that it undergoes a stepwise decomposition on heating. The decomposition starts with the gradual loss of structural and surface water (≈ 14.4 wt%) up to 220 °C, beyond which the classical sequential decomposition of CaOx to $CaCO_3$ (weight loss of 15.5 wt% up to 470 °C) and calcium oxide (weight loss of 29.2 wt% up to 630°C) is observed.[47] The recorded amount of calcium carbonate formed and the weight loss associated with H_2O loss yield a composition of the prepared ACO of ≈ CaC_2O_4:H_2O. Simultaneous differential scanning calorimetry (DSC) was also performed with the TGA but did not detect an amorphous to crystalline transition for the ACO; a similar observation is also commonly made for ACC formed at lower pH levels.[48] The stepwise weight loss transitions from hydrated ACO to CaOx and $CaCO_3$ are in good agreement with (varying by ≈ 5%) the theoretical values predicted for idealized molecular compositions, while the final transformation of $CaCO_3$ to CaO varied by up to 15% from the theoretical value. This likely derives from the silica impurity observed in the IR spectrum of the ACO produced by freeze concentration, although every reasonable effort (including the use of Teflon vessels) was made to avoid this. Typical weight loss profiles of COM and COD are presented in Supporting Figure 4.

DISCUSSION

While crystallization has been studied for centuries – using traditional methods such as optical microscopy – recent advances in analytical techniques that enable characterization of the nanoscale processes which govern crystal nucleation and growth have fuelled a resurgence of interest in this fascinating topic. For example, it is now recognized that crystal growth frequently occurs by the assembly of species ranging from clusters to crystalline nanoparticles rather than ion-by-ion growth,[49] and that nucleation itself may proceed via the aggregation of clusters and complexes.[50, 51] The observation that crystalline calcium carbonate biominerals can form via amorphous calcium carbonate also raised interest in this process and inspired researchers to investigate the generality of this potential crystallization mechanism. However, while a large number of insoluble minerals are now known to crystallize via this route,[52] our work is the first to clearly demonstrate that calcium oxalate can also precipitate via an amorphous phase from aqueous solution. It is therefore valuable to consider why ACO has proven so difficult to observe and isolate as compared with amorphous calcium carbonate and amorphous calcium phosphate, which have both been recognized for some time.[53, 54]

One factor that clearly contributes to the difficulty in observing ACO is the sensitivity of calcium oxalate precipitates to radiation/ electron beam damage and is subsequent decomposition/ transformation.[33] Prolonged electron beam exposure of calcium oxalate crystals is known to either yield feature less electron diffraction pattern or diffraction pattern corresponding to calcite or calcium oxide.[55] We can also speculate that the kinetic barriers associated with the formation of ACO and COM/ COD may be much more similar in magnitude than those between amorphous calcium carbonate and calcite/ vaterite (crystalline $CaCO_3$ polymorphs); metastable polymorphs typically form when the kinetic barriers to their formation are significantly less than those of more stable polymorphs (Ostwald's rule of stages). In this case, the calcium oxalate system would have "less to gain" by forming an amorphous precursor phase than the calcium carbonate system. This possibility is also supported by our observation that ACO and COM are very similar in composition ($\approx CaC_2O_4{:}H_2O$), while amorphous calcium carbonate has a typical composition of $CaCO_3{:}H_2O$, as compared with the anhydrous crystalline polymorphs calcite, vaterite and aragonite.

CONCLUSIONS

The work presented here provides strong evidence that crystalline calcium oxalate can precipitate via an amorphous precursor phase in aqueous solution. Particles of size 10-50 nm and compositions $\approx CaC_2O_4{:}H_2O$ were identified, although these were always present in combination with crystalline particles when precipitated from bulk solution. Use of a freeze concentration method enabled significant quantities of pure ACO to be generated for structural and compositional analysis. Our experiments also demonstrate that ACO can be significantly stabilized within confined volumes, where these were here provided by a crossed cylinders apparatus and track-etched membrane pores. The stabilization of metastable phases in confinement has now been observed for quite a number of insoluble minerals (calcium carbonate, calcium sulfate and calcium phosphate),[11, 28, 29, 44, 45] indicating that this may be a widespread phenomenon. At the length scales involved in these experiments, this effect can again be ascribed to kinetic factors, and may originate from a number of phenomena such as the slower transport of ions between a dissolving metastable phase, and the more stable, growing phase, the elimination of impurities and hindered aggregation of precursor particles. It is also noteworthy that soluble additives and confinement effects – which are both characteristic of biomineralization processes – can act synergistically to give greatly enhanced stability of

metastable phases. These results therefore suggest that crystalline calcium oxalate biominerals may form via an amorphous phase, but that the relatively short lifetime of this material when precipitated in bulk and the challenges associated with identifying amorphous phases when they are present in combination with crystalline ones has to date limited its identification. Further work is therefore required to fully characterize calcium oxalate biominerals and their formation mechanisms.

EXPERIMENTAL SECTION

Materials. $CaCl_2$:$2H_2O$, $Na_2C_2O_4$, CaC_2O_4 (99.999%) and Poly acrylic acid (PAA) average M_w ≈5,100 were purchased from Sigma-Aldrich and used as received. Aqueous solutions were prepared using Milli-Q Standard or double distilled water. Glassware was soaked overnight in 10% w/v NaOH, followed by rinsing with dilute HCl and finally washing with Milli-Q water. Glass slides and crystallizing dishes were placed overnight in Piranha solution (70:30 wt% sulfuric acid: hydrogen peroxide) and were then washed copiously with Milli-Q water before use. Crystallization solutions were degassed with nitrogen for 2 hours prior to use to avoid the possible formation of $CaCO_3$.

Bulk precipitation of calcium oxalate (CaOx). Bulk precipitation of calcium oxalate was induced by the direct combination of equimolar solutions of $CaCl_2$ and $Na_2C_2O_4$ (0.25-100 mM), where these have pH values of 5.1-6.6 and 7.5-7.9, respectively. The known calcium oxalate crystal growth retarder (PAA) was added to the oxalate solution. The precipitate formed was then isolated by filtering the solution using a 0.45-µm Isopore GTTP membrane filter (Millipore) and was washed with ethanol before being left to dry. Piranha cleaned glass substrates were also placed at the base of crystallization dishes, and were removed from the solution after precipitation had occurred. The glass substrates supporting CaOx crystals were washed with ethanol and left to dry before analysis.

Calcium oxalate precipitated in a crossed cylinders apparatus.[11] Glass tubes with diameters of 25 mm were cut to produce 25 mm long half-cylinders. The half-cylinders were cleaned by immersing them in Piranha solution overnight, followed by rinsing with Millipore (18.2 MΩ) water and ethanol, and drying with nitrogen gas. The glass cylinders were mounted in Teflon holders to hold them in place. A TEM grid was placed between the two glass cylinders before brought into contact with the curved surfaces facing each other. A spring and metal screws on the top of the holder provide a slowly increasing force that brings the glass surfaces/ TEM grid gently into contact. CaOx precipitation was initiated around the contact point of the two half cylinders by adding 20 µl of a freshly prepared metastable crystal growth solution between the cylinders. The metastable crystal growth solution was prepared by combining 10 µl volumes of $CaCl_2$ and $Na_2C_2O_4$ solutions of concentrations 2 mM and pH values 6.45 and 7.8 respectively.

Precipitation in track-etch membrane pores. Calcium oxalate was precipitated within the 200 nm pores of polycarbonate track-etch membranes (Isopore, Millipore). Membranes were initially plasma cleaned and then degassed in water at reduced pressure to ensure complete filling of the membrane pores with solution. In the used double diffusion (U-tube) method,[34] wetted membranes

are mounted between two U-tube arms which are then filled with solutions of $CaCl_2$ (2 - 10 mM / ≈ pH 6.3) and $Na_2C_2O_4$ (2 - 10 mM)/ PAA (100 μg ml^{-1} / ≈ pH 7.6). Intra-membrane particles were isolated either after 12 hours or 2 weeks by dissolution of the membranes in dichloromethane. After precipitation, membranes were rinsed with ethanol, their surfaces were scraped with a cover glass and they were then wiped with filter paper to remove the majority of surface-bound crystals. The membranes were then subjected to at least 3 cycles of sonication in dichloromethane/ centrifugation and exchange of the solvent for fresh. The isolated precipitates were rinsed with methanol to remove residual dichloromethane, and were finally washed with ethanol before being pipetted onto a TEM grid/ glass for analysis.

Calcium oxalate precipitation via freeze concentration.[26] Calcium oxalate produced by freeze-drying requires the production of "counter-ion free", saturated CaC_2O_4 solutions. "Pure" solid CaC_2O_4 was used as a starting reagent and the entire process was performed in Teflon vessels to prevent silica contamination arising from dissolution of glassware. Saturated solutions were prepared by adding 20 mg of "pure" CaC_2O_4 to 500 ml DI water, and were stored for 24 hours at room temperature before centrifuging to remove the majority of any remaining un-dissolved calcium oxalate. This saturated solution was then briefly heated (50°C) to remove possible ghost nuclei, and was then filtered through a 0.2 μm membrane filter. Freezing of the prepared saturated solutions, (5 - 40 ml), was achieved by plunge immersion into a liquid nitrogen bath, followed by a 10 minute annealing period to strengthen the ice structure. Subsequent sublimation (Labcono FreezeZone 1, 50 mBar, -49°C) of the excess solvent delivers the freeze-dried calcium oxalate.

Characterization. Crystal morphologies were determined using scanning electron microscopy (SEM) and transmission electron microscopy (TEM). Samples were mounted using adhesive conducting pads or transferred onto gold or copper grids. SEM images were acquired using a FEI Nova NanoSEM 650, TEM images and electron diffraction patterns were acquired using a FEI Tecnai F20 - 200 kV FEG-TEM fitted with an Oxford Instruments INCA 350 EDX system/80mm X-Max SDD detector and a Gatan Orius SC600A CCD camera. Low dose TEM and low dose selected area electron diffraction (SEAD) were recorded with an electron dose < 100 electrons /$Å^2$. These experiments were performed using a FEI Tecnai 20 (type sphera) microscope operating at 200 kV with a LaB_6 filament and a bottom mounted 1024 x 1024 Gatan msc 794™ CCD camera (Figure 4c,d-l*,* Supporting Figure 3) or on the TU/e cryoTITAN (FEI, www.cryotem.nl) operated at 300 kV, equipped with a field emission gun (FEG), a post-column Gatan Energy Filter (GIF), using a pre-GIF gatan 2k x 2k gatan CCD camara for diffraction (Figure 4c-*ii*) and a post-GIF 2k x 2k Gatan CCD camera for imaging (Figure 4d-

ii). Crystal polymorphs were also determined by Raman microscopy, using a Renishaw 2000 inVia-Raman microscope equipped with a 785 nm diode laser or with IR spectroscopy, using a Perkin Elmer Spectrum 100 FT-IR Spectrometer. The composition of the formed ACO was investigated using TGA, where data were recorded using a TA Instruments STD Q600, with a heating rate of 15 °C min^{-1} under 100 ml min^{-1} N_2 flow.

AUTHOR INFORMATION

Corresponding Authors

*Fiona C. Meldrum, e-mail: F.Meldrum@leeds.ac.uk

*Johannes Ihli, e-mail: cmjfi@leeds.ac.uk

ACKNOWLEDGEMENTS

This work was supported by an Engineering and Physical Sciences Research Council (EPSRC) Leadership Fellowship (F.C.M., J.I., Y. W. W and Y-Y.K., EP/H005374/1) and an EPSRC Programme Grant (DCG and FCM, EP/I001514/1) which funds the Materials in Biology (MIB) consortium. It was also supported by the European Community FP6, project code NMP4-CT-2006-033277 (PHHB and NAJMS). We would also like to thank Lia Addadi and Assaf Gal for experimental suggestions.

SUPPORTING INFORMATION

Additional characterization of the calcium oxalate precipitates is provided. This information is available free of charge via the Internet at http: //pubs.acs.org.

NOTES

The authors declare no competing financial interests.

REFERENCES

1. Meldrum, F. C.; Colfen, H., Controlling Mineral Morphologies and Structures in Biological and Synthetic Systems *Chem. Rev.* **2008,** *108*, 4332.

2. Addadi, L.; Raz, S.; Weiner, S., Taking Advantage of Disorder: Amorphpous Clacium Carbonate and its Roles in Biomineralization *Adv. Mater.* **2003,** *15*, 959.

3. Weiss, I. M.; Tuross, N.; Addadi, L.; Weiner, S., Mollusc larval shell formation: amorphous calcium carbonate is a precursor phase for aragonite *J. Exp. Zool.* **2002,** *293*, 478.

4. Beniash, E.; Metzler, R. A.; Lam, R. S. K.; Gilbert, P. U. P. A., Transient amorphous calcium phosphate in forming enamel *J. Struct. Biol.* **2009,** *166*, 133.

5. Mahamid, J.; Sharir, A.; Addadi, L.; Weiner, S., Amorphous calcium phosphate is a major component of the forming fin bones of zebrafish: Indications for an amorphous precursor phase *Proc. Natl. Acad. Sci. U. S. A.* **2008,** *105*, 12748.

6. Gal, A.; Brumfeld, V.; Weiner, S.; Addadi, L.; Oron, D., Certain Biominerals in Leaves Function as Light Scatterers *Adv. Mater.* **2012,** *24*, OP77.

7. Baumgartner, J.; Morin, G.; Menguy, N.; Perez Gonzalez, T.; Widdrat, M.; Cosmidis, J.; Faivre, D., Magnetotactic bacteria form magnetite from a phosphate-rich ferric hydroxide via nanometric ferric (oxyhydr)oxide intermediates *Proc. Natl. Acad. Sci. U. S. A.* **2013,** *110*, 14883.

8. Tiemann, H.; Sotje, I.; Jarms, G.; Paulmann, C.; Epple, M.; Hasse, B., Calcium sulfate hemihydrate in statoliths of deep-sea medusae *J. Chem. Soc.-Dalton Trans.* **2002**, 1266.

9. Kabalah-Amitai, L.; Mayzel, B.; Kauffmann, Y.; Fitch, A. N.; Bloch, L.; Gilbert, P. U. P. A.; Pokroy, B., Vaterite Crystals Contain Two Interspersed Crystal Structures *Science* **2013,** *340*, 454.

10. Mann, S., *Biomineralization: Principles and Concepts in Bioinorganic Materials Chemistry*. Oxford University Press: Oxford, U.K., 2001; p 240.

11. Stephens, C. J.; Ladden, S. F.; Meldrum, F. C.; Christenson, H. K., Amorphous Calcium Carbonate is Stabilised in Confinement *Adv. Func. Mater.* **2010,** *20*, 2108.

12. Schenk, A. S.; Albarracin, E. J.; Kim, Y.-Y.; Ihli, J.; Meldrum, F. C., Confinement stabilises single crystal vaterite rods *Chem. Commun.* **2014,** *50*, 4729.

13. Nudelman, F.; Sonmezler, E.; Bomans, P. H. H.; de With, G.; Sommerdijk, N. A. J. M., Stabilization of amorphous calcium carbonate by controlling its particle size *Nanoscale* **2010,** *2*, 2436.

14. Wallace, A. F.; Hedges, L. O.; Fernandez-Martinez, A.; Raiteri, P.; Gale, J. D.; Waychunas, G. A.; Whitelam, S.; Banfield, J. F.; De Yoreo, J. J., Microscopic Evidence for Liquid-Liquid Separation in Supersaturated $CaCO_3$ Solutions *Science* **2013,** *341*, 885.

15. Nancollas, G. H.; Reddy, M. M.; Tsai, F., Calcium Sulfate Dihydrate Crystal - Growth in Aqueous Solution at Elevated Temperatures *J. Cryst. Growth* **1973,** *20*, 125.

16. Furby, E.; Glueckau, E.; McDonald, L. A., Solubility of Calcium Sulphate in Sodium Chloride and Sea Salt Solutions *Desalination* **1968,** *4*, 264.

17. Wang, Y.-W.; Kim, Y.-Y.; Christenson, H. K.; Meldrum, F. C., A new precipitation pathway for calcium sulfate dihydrate (gypsum) via amorphous and hemihydrate intermediates *Chem. Commun.* **2012,** *48*, 504.

18. Webb, M. A., Cell-Mediated Crystallization of Calcium Oxalate in Plants *Plant Cell* **1999,** *11*, 751.

19. Zindler-Frank, E.; Hönow, R.; Hesse, A., Calcium and oxalate content of the leaves of Phaseolus vulgaris at different calcium supply in relation to calcium oxalate crystal formation *Plant Physiol.* **2001,** *158*, 139.

20. Brubaker, C. L.; Horner, H. T., Development of epidermal crystals in leaflets of Stylosanthes guianensis (Leguminosae; Papilionoideae) *Botany* **1989,** *67*, 1664.

21. Franceschi, V. R.; Nakata, P. A., Calcium Oxalate in Plants: Formation and Function *Annu. Rev. Plant Biol.* **2005,** *56*, 41.

22. Franceschi, V. R.; Horner, H. T., Calcium Oxalate Crystals in Plants *Botanical Rev.* **1980,** *46*, 361.

23. Wang, L. J.; Qiu, S. R.; Zachowicz, W.; Guan, X. Y.; DeYoreo, J. J.; Nancollas, G. H.; Hoyer, J. R., Modulation of calcium oxalate crystallization by linear aspartic acid-rich peptides *Langmuir* **2006,** *22*, 7279.

24. Colas, H.; Bonhomme-Coury, L.; Diogo, C. C.; Tielens, F.; Babonneau, F.; Gervais, C.; Bazin, D.; Laurencin, D.; Smith, M. E.; Hanna, J. V.; Daudon, M.; Bonhomme, C., Whewellite, CaC2O4 center dot H2O: structural study by a combined NMR, crystallography and modelling approach *Crystengcomm* **2013,** *15*, 8840.

25. Hajir, M.; Graf, R.; Tremel, W., Stable amorphous calcium oxalate: Synthesis and potential intermediate in biomineralization *Chem. Commun.* **2014,** *50*, 6534.

26. Ihli, J.; Kulak, A. N.; Meldrum, F. C., Freeze-drying yields stable and pure amorphous calcium carbonate (ACC) *Chem. Commun.* **2013,** *49*, 3134.

27. Stephens, C. J.; Kim, Y.-Y.; Evans, S. D.; Meldrum, F. C.; Christenson, H. K., Early Stages of Crystallization of Calcium Carbonate Revealed in Picoliter Droplets *J. Am. Chem. Soc.* **2011,** *133*, 5210.

28. Cantaert, B.; Beniash, E.; Meldrum, F. C., Nanoscale Confinement Controls the Crystallization of Calcium Phosphate: Relevance to Bone Formation *Chem. Eur. J.* **2013,** *19*, 14918.

29. Tester, C. C.; Whittaker, M. L.; Joester, D., Controlling nucleation in giant liposomes *Chem. Commun.* **2014,** *50*, 5619.

30. Gower, L. B.; Odom, D. J., Deposition of calcium carbonate films by a polymer-induced liquid-precursor (PILP) process *J. Cryst. Growth* **2000,** *210*, 719.

31. Cantaert, B.; Kim, Y.-Y.; Ludwig, H.; Nudelman, F.; Sommerdijk, N. A. J. M.; Meldrum, F. C., Think Positive: Phase Separation Enables a Positively Charged Additive to Induce Dramatic Changes in Calcium Carbonate Morphology *Adv. Func. Mater.* **2012,** *22*, 907.

32. Schenk, A. S.; Zope, H.; Kim, Y.-Y.; Kros, A.; Sommerdijk, N. A. J. M.; Meldrum, F. C., Polymer-induced liquid precursor (PILP) phases of calcium carbonate formed in the presence of synthetic acidic polypeptides-relevance to biomineralization *Farad. Discuss.* **2012,** *159*, 327.

33. Crawford, D., Electron microscopy of urinary calculi — Some facts and artefacts *Urol. Res.* **1984,** *12*, 17.

34. Kim, Y.-Y.; Hetherington, N. B. J.; Noel, E. H.; Kröger, R.; Charnock, J. M.; Christenson, H. K.; Meldrum, F. C., Capillarity Creates Single-Crystal Calcite Nanowires from Amorphous Calcium Carbonate *Angew. Chem.-Int. Edit.* **2012,** *50*, 12572.

35. Rodriguez-Blanco, J. D.; Shaw, S.; Benning, L. G., How to make 'stable' ACC: protocol and preliminary structural characterization *Mineral. Mag.* **2008,** *72*, 283.

36. Conti, C.; Casati, M.; Colombo, C.; Realini, M.; Brambilla, L.; Zerbi, G., Phase transformation of calcium oxalate dihydrate–monohydrate: Effects of relative humidity and new spectroscopic data *Spectrochim. Acta Mol. Biomol. Spectros.* **2014,** *128*, 413.

37. Davey, R. J.; Cardew, P. T.; McEwan, D.; Sadler, D. E., Rate controlling processes in solvent-mediated phase transformations *J. Cryst. Growth* **1986,** *79*, 648-653.

38. Doherty, W. O. S.; Fellows, C. M.; Gorjian, S.; Senogles, E.; Cheung, W. H., Inhibition of calcium oxalate monohydrate by poly(acrylic acid)s with different end groups *J. Appl. Polym. Sci.* **2004,** *91*, 2035.

39. Farmanesh, S.; Ramamoorthy, S.; Chung, J.; Asplin, J. R.; Karande, P.; Rimer, J. D., Specificity of Growth Inhibitors and their Cooperative Effects in Calcium Oxalate Monohydrate Crystallization *J. Am. Chem. Soc.* **2013,** *136*, 367.

40. Kleinman, J. G.; Alatalo, L. J.; Beshensky, A. M.; Wesson, J. A., Acidic polyanion poly(acrylic acid) prevents calcium oxalate crystal deposition *Kidney Int.* **2008,** *74*, 919.

41. Gower, L. B., Biomimetic Model Systems for Investigating the Amorphous Precursor Pathway and Its Role in Biomineralization *Chem. Revs.* **2008,** *108*, 4551.

42. Cantaert, B.; Verch, A.; Kim, Y.-Y.; Ludwig, H.; Paunov, V. N.; Kroeger, R.; Meldrum, F. C., Formation and Structure of Calcium Carbonate Thin Films and Nanofibers Precipitated in the Presence of Poly(Allylamine Hydrochloride) and Magnesium Ions *Chem. Mater.* **2013,** *25*, 4994.

43. Bewernitz, M. A.; Gebauer, D.; Long, J.; Colfen, H.; Gower, L. B., A metastable liquid precursor phase of calcium carbonate and its interactions with polyaspartate *Farad. Discuss.* **2012,** *159*, 291.

44. Wang, Y.-W.; Christenson, H. K.; Meldrum, F. C., Confinement Leads to Control over Calcium Sulfate Polymorph *Adv. Func. Mater.* **2013,** *23*, 5615.

45. Wang, Y.-W.; Christenson, H. K.; Meldrum, F. C., Confinement Increases the Lifetimes of Hydroxyapatite Precursors *Chem. Mater.* **2014,** *26*, 5830.

46. Loste, E.; Meldrum, F. C., Control of calcium carbonate morphology by transformation of an amorphous precursor in a constrained volume *Chem. Commun.* **2001**, 901.

47. Kociba, K. J.; Gallagher, P. K., A study of calcium oxalate monohydrate using dynamic differential scanning calorimetry and other thermoanalytical techniques *Thermochim. Acta* **1996,** *283*, 277.

48. Koga, N.; Nakagoe, Y.; Tanaka, H., Crystallization of amorphous calcium carbonate *Thermochim. Acta* **1998,** *318*, 239.

49. Penn, R. L.; Banfield, J. F., Imperfect oriented attachment: Dislocation generation in defect-free nanocrystals *Science* **1998,** *281*, 969.

50. Gebauer, D.; Kellermeier, M.; Gale, J. D.; Bergstrom, L.; Colfen, H., Pre-nucleation clusters as solute precursors in crystallisation *Chem. Soc. Rev.* **2014,** *43*, 2348.

51. Habraken, W.; Tao, J. H.; Brylka, L. J.; Friedrich, H.; Bertinetti, L.; Schenk, A. S.; Verch, A.; Dmitrovic, V.; Bomans, P. H. H.; Frederik, P. M.; Laven, J.; van der Schoot, P.; Aichmayer, B.; de With, G.; DeYoreo, J. J.; Sommerdijk, N., Ion-association complexes unite classical and non-classical theories for the biomimetic nucleation of calcium phosphate *Nat. Commun.* **2013,** *4*, 12.

52. Wolf, S. E.; Muller, L.; Barrea, R.; Kampf, C. J.; Leiterer, J.; Panne, U.; Hoffmann, T.; Emmerling, F.; Tremel, W., Carbonate-coordinated metal complexes precede the formation of liquid amorphous mineral emulsions of divalent metal carbonates *Nanoscale* **2011,** *3*, 1158.

53. Hunt, T. S., On some reactions of the salts of lime and magnesia *Amer. J. Sci. Arts* **1859,** *28*, 170

54. Wang, L.; Li, S.; Ruiz-Agudo, E.; Putnis, C. V.; Putnis, A., Posner's cluster revisited: direct imaging of nucleation and growth of nanoscale calcium phosphate clusters at the calcite-water interface *CrystEngComm* **2012,** *14*, 6252.

55. Rao, M. V. R.; Chhotray, N.; Agarwal, J. S., Studies on the morphology and electron beam induced phase transformation of calcium oxalate monohydrate *J. Cryst. Growth* **1986,** *74*, 139.

Table of Contents: